

Optics Letters

Compact 3–8 μm supercontinuum generation in a low-loss As_2Se_3 step-index fiber

LOUIS-RAFAËL ROBICHAUD,^{1,2,*} VINCENT FORTIN,¹ JEAN-CHRISTOPHE GAUTHIER,¹ STÉPHANE CHÂTIGNY,² JEAN-FRANÇOIS COUILLARD,² JEAN-LUC DELAROSBIL,² RÉAL VALLÉE,¹ AND MARTIN BERNIER¹

¹Center for Optics, Photonics and Lasers (COPL), Université Laval, Québec G1 V 0A6, Canada

²CorActive High-Tech Inc., Québec G2C 1S9, Canada

*Corresponding author: louis-rafael.robichaud.1@ulaval.ca

Received 18 July 2016; revised 29 August 2016; accepted 3 September 2016; posted 6 September 2016 (Doc. ID 270794); published 3 October 2016

A mid-infrared supercontinuum source spanning from 3 to 8 μm is demonstrated using a low-loss As_2Se_3 commercial step-index fiber. A maximum average output power of 1.5 mW is obtained at a low repetition rate of 2 kHz. Thanks to the low NA step-index fiber, the output is single mode for wavelengths above $\sim 5 \mu\text{m}$. The pump source consists of an erbium-doped ZrF_4 -based in-amplifier supercontinuum source spanning from 3 to 4.2 μm . The effects of both the pump power and As_2Se_3 fiber length on the output characteristics are studied. To the best of our knowledge, this is the first compact supercontinuum source ever reported to reach 8 μm in a standard step-index fiber. © 2016 Optical Society of America

OCIS codes: (060.4370) Nonlinear optics, fibers; (320.6629) Supercontinuum generation; (060.2320) Fiber optics amplifiers and oscillators; (060.2390) Fiber optics, infrared; (140.3070) Infrared and far-infrared lasers.

<http://dx.doi.org/10.1364/OL.41.004605>

Mid-infrared (mid-IR) light sources have been the subject of a sustained research effort driven by vast potential applications in the molecular fingerprint region (~ 3 to 20 μm). Supercontinuum (SC) sources are set to have a significant impact in many applications [1,2] because they combine the brightness of fiber lasers with the extremely wide spectral coverage of blackbody radiation.

SC sources can be conveniently classified based on four specific practical features: (1) the output characteristics (average output power, spectral bandwidth, and degree of coherence), (2) the pumping source (optical parametric oscillator/amplifier [OPO/OPA] or fiber based), (3) the waveguide profile (low NA [i.e., <0.5] step-index fiber [SIF], high NA step-index fiber [HNASIF], or microstructured optical fiber [MOF]), and (4) the nonlinear material (oxide, fluoride, or chalcogenide [ChG] glasses). The most studied glasses for SC generation, as well as their infrared transparency limit at the 1 dB/m level, are silicate glasses (2.4 μm), zirconium fluoride glasses (ZFG) (4.3 μm), indium fluoride glasses (IFG) (5.4 μm), and ChG

glasses such as AsS (7 μm) and AsSe (9 μm) [3]. ChGs are currently the only choice to extend the SC beyond 5.5 μm in meter-long fibers and are very efficient material candidates for this purpose, given their very high nonlinearity. For example, the nonlinear refractive index of AsSe is about 600 times higher than that of silica-based glasses [3]. ChG SIFs also recently were proven to be suitable for SC generation at a watt-level output power near 2 μm [4], a demonstration that gives confidence in the robustness of these fibers.

The state-of-the-art approach to obtain the broadest mid-IR spectrum relies on pumping with an OPO/OPA source in very short pieces of HNASIF ChG fibers (typically less than 15 cm in length) [5–8] with a pump wavelength in the anomalous dispersion regime of the nonlinear fiber. So far, the broadest SC ever reported spread from 2 to 15.1 μm [5] but exhibited a very low average output power (at the microwatt level) due to the low intrinsic repetition rate of the pump source. On the other hand, since OPO/OPA-based mid-IR SCs are typically expensive and cumbersome, they are generally not appropriate for practical applications. Consequently, there is a need for better strategies to deliver SC output with high performance in a compact package.

Fiber-based SC generation, i.e., based on fiber laser/amplifier pumping source, provides a potentially robust, compact, and low-cost solution to solve this issue. The common solution is to use mature near-infrared fiber lasers as pump sources, namely around 1.55 and 2 μm , and concatenate silica with fluoride and/or ChG fibers to redshift the spectrum. Gattass *et al.* recently reported an experimental SC spanning from 1.9 to 4.8 μm from a multistage amplifier (Er/Yb and Tm) and a silica–AsS cascade [8]. Very recently, a SC extending up to 7.0 μm was pumped with amplified nanosecond pulses that were spectrally broadened in a ZBLAN–AsSe cascade [9]. In this report, the nonlinear medium used was a ChG MOF, despite their associated key issues such as low mechanical robustness [9] and environmental degradation [10]. Recently, Gauthier *et al.* proposed a promising approach for efficiently producing a mid-IR SC directly in-amplifier with a proof-of-concept SC spanning from 2.7 to 4.2 μm [11], limited by the transparency of the Er^{3+} :ZFG fiber. An even broader SC spanning from 2.4 to 5.4 μm was further

demonstrated using a low-loss IFG fiber [12], again limited by the transparency of the fiber.

In this Letter, we report a compact mid-IR SC spanning from 3 to 8 μm based on a low-loss AsSe SIF (CorActive IRT-SE-18/170) and pumped with an in-amplifier SC source extending up to 4.2 μm . The best SC performances were obtained with a fiber length of 3.5 m, leading to an average output power of 1.5 mW and theoretical single-mode operation from 5.2 to 8 μm .

The schematic of the experimental setup is presented in Fig. 1. The reader is referred to Ref. [11] for details on optical components from the optical parametric generation (OPG) seed source to the end of the erbium-doped ZFG. The main difference from the original scheme is that both the seed (2.8 μm , 400 ps, 2 kHz) and the pump (980 nm, CW) are co-propagating in the fiber amplifier. An amplifier length of 5.5 m was used to generate the in-amplifier SC used in this experiment. The amplifier output, ranging from 2.6 to 4.2 μm , was then filtered using a long-pass filter (LPF) with a cutoff wavelength of 3 μm to prevent damage to the ChG fiber tip as well as parasitic CW lasing from the amplifier. This filter was placed between a pair of antireflection (AR)-coated (3–5 μm) aspheric ZnSe lenses, each having a 12.7 mm focal length. Each lens resulted in a $\sim 3\%$ loss due to absorption and residual reflection of the coating, while the filter had a transmission loss of about 15% above 3 μm . The filtered spectrum was then launched into an undoped single-mode ZFG SIF with a measured efficiency of 55%. This fiber was used as a spatial filter to provide a single-mode output beam with a low NA (0.12) for efficient coupling into the ChG SIF ($\sim 75\%$ coupling, excluding Fresnel reflections) in order to increase both the damage threshold and the launching stability. An indium–gallium alloy was applied on both AsSe fiber ends to remove the cladding modes. All the fibers used in this experiment have a step-index profile. Table 1 summarizes the key parameters for these fibers, while Fig. 2 shows the ChG SIF cleaved face along with its attenuation and dispersion curves.

The ChG SIF propagation losses were measured following a standard cut-back procedure with a Fourier-transform infrared spectroscopy system (Hamilton Sundstrand, Analect Diamond 20), which is illuminated by a heated filament. This fiber displays a low background loss between 2 and 7 μm (with a minimum loss of 0.1 dB/m at 4.1 μm). A multistep purification process was done to reduce its O–H and Se–H absorption peaks below 0.5 dB/m at, respectively, 2.9 and 4.6 μm . The long

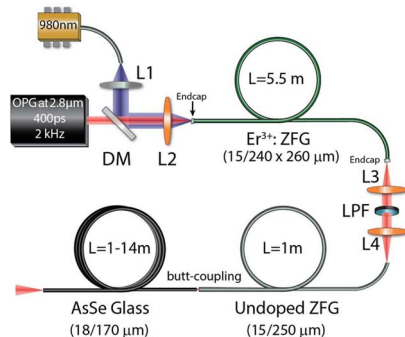


Fig. 1. Schematic of the experimental setup. L1, silica lens; L2–L4, ZnSe aspheric lenses; DM, dichroic mirror with high reflection (HR) at 980 nm, high transmission (HT) at 2800 nm; LPF, long-pass filter with cutoff wavelength at 3 μm (-3 dB level).

Table 1. Fiber Parameters Summary^a

Parameter	EDFF	UFF	ChG SIF
Core material	Er ³⁺ (7%):ZFG	ZFG	As _{35.6} Se _{64.4}
Clad material	ZFG	ZFG	As ₃₅ Se ₆₅
NA (—)	0.12	0.12	0.22
Core diam. (μm)	15	15	18
Clad diam. (μm)	240 \times 260	250	170
ZDW (μm)	1.6 [13]	1.6 [13]	7
Cutoff (μm)	2.5	2.5	5.2
Length (m)	5.5	1.1	Up to 30
Manufacturer	LVF	LVF	CorActive

^aEDFF, erbium-doped fluoride fiber; UFF, undoped fluoride fiber; LVF, Le Verre Fluoré.

wavelength transmission of the SIF is ultimately limited to ~ 8 μm due to confinement losses (e.g., bending losses) resulting from the ~ 5 μm cutoff wavelength of the fiber (mode area of 608 μm^2 at 8 μm versus 284 μm^2 at 5 μm). In comparison, a multimode AsSe SIF (CorActive IRT-SE 100/170) produced with the same glasses demonstrated a transmission capability up to 9 μm (at 1 dB/m) [14]. Despite this 8 μm edge, the attenuation curve presented in Fig. 2 is among the best ever reported for an AsSe SIF.

The computation of the ChG refractive index is based on the Sellmeier equation with the coefficients found in Ref. [15]. The index profile is evaluated for the As₃₅Se₆₅ clad composition by extrapolation. The ChG SIF NA was deduced from an experimental measure of the far-field intensity profile at 1550 nm using a goniometer. The refractive index profile of the fiber was obtained from the measured NA, and the core size was evaluated with a calibrated microscope after etching the tip with KOH (see inset of Fig. 2). This chemical etching process enhances the core/clad interface visibility, but it also increases the surface roughness. The dispersion curve of the fundamental mode was calculated with the Mode Solutions software from Lumerical Inc. [16]. The ZDW is expected to be near 8.9 μm , slightly redshifted compared to that of the stoichiometric As₄₀Se₆₀ glass composition.

The measurement setup includes a thermopile detector (Gentec EO, XLP12-3S-H2) to record each SC average output

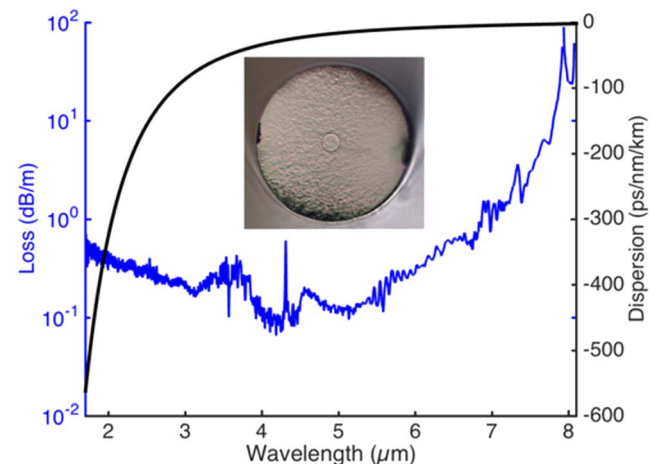


Fig. 2. Background losses (solid blue curve) and dispersion curve of the ChG SIF. The inset shows an image of the ChG fiber cleaved face after KOH etching to enhance the core/clad interface visibility.

power. The output SC spectra were measured by a spectrometer composed of a monochromator (Digikrom, DK480) and a liquid-nitrogen-cooled mercury cadmium telluride (MCT) detector (Judson, J15D12-M204-S01M-60), providing 2.5–12 μm measurement capability. The system was calibrated by comparing the measured blackbody (OceanOptics, CoolRed) radiation to the corresponding theoretical curve. A set of high-pass filters were properly used to avoid any overlap with lower wavelength light by the higher diffraction orders of the monochromator. For all the measurements, the resolution of the spectral monitoring system was set to 10 nm. The spectra were normalized in dBm/nm according to their measured average output power.

The in-amplifier SC evolution (after filtering with the 3 μm cutoff long-pass filter) measured at the output of the undoped ZFG fiber is presented in Fig. 3 for several launched pump powers. As expected, the total output power increases with the pump power, while the output spectrum is asymmetrically broadened toward the longer wavelengths. Indeed, the ZFG multiphonon absorption edge is located near 4.2 μm , which limits further spectral broadening from the source above a launched 980 nm pump power of about 1 W. Therefore, further increase in the pumping level has practically no influence on the in-amplifier SC spectrum (see Fig. 3), apart from generating slightly more average output power. On the short wavelength side (near 3 μm), the SC is limited by the long-pass filter. Without this filter, the SC spectrum spreads from 2.6 to 4.2 μm with a maximum output power of 27.2 mW (at 0.82 W pump power). It is also important to mention that the propagation inside of the undoped ZFG did not affect the in-amplifier SC spectrum in terms of shape and spectral width.

Figures 4 and 5 show the effect of fiber length on the ChG output spectrum and average power for a pump power of 0.82 W. We note that only 1 m is sufficient for the SC's edge to reach 6 μm and surpass the transparency window of fluoride fibers. Since the fiber exhibit an all-normal dispersion up to ~ 8.9 μm , the spectrum broadens mainly through self-phase modulation (SPM). Therefore, unlike SC sources operating in the anomalous regime (i.e., dominated by soliton fission and Raman self-frequency shift processes; see Ref. [12] for instance), the spectra measured in this experiment have a much smoother

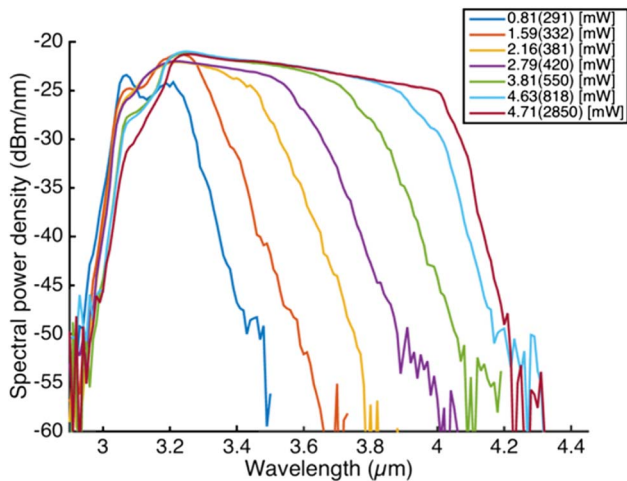


Fig. 3. Undoped ZFG output spectrum evolution for several average output powers. The corresponding launched pump powers are shown in parentheses. Spectral resolution was set to 10 nm.

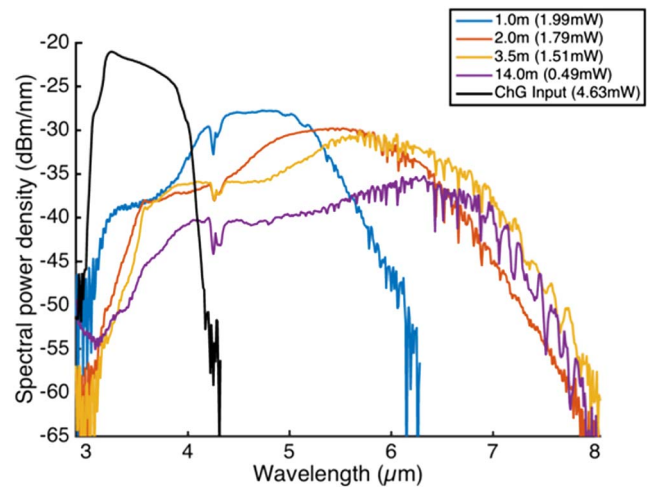


Fig. 4. Evolution of the output SC spectrum generated with different fiber lengths at a pump power of 0.82 W. The corresponding average output powers are shown in parentheses. ChG input refers to the SC spectrum launched into the AsSe SIF.

shape. The asymmetry of the spectra toward longer wavelengths isn't fully understood, but it may be the result of intrapulse Raman scattering, which also explains the SC redshifting with longer fiber lengths. Figure 5 presents the ChG output/input power ratio with respect to fiber length. These results indicate that the total output power decreases significantly over the first 9 m of ChG fiber. This is explained by the sharp increase of fiber propagation losses once the spectrum extends beyond 6 μm (see Fig. 2). For ChG fiber lengths beyond 9 m, the losses steadily converge since the broadening of the spectrum ceases.

An optimal fiber length of 3.5 m is estimated based on the best spectral coverage and average power characteristics. For shorter fiber lengths, the SC isn't completely redshifted and, above 3.5 m, background losses take over and reduce the overall SC power density, as discussed above. Note that the CO₂ absorption peak can be seen near 4.3 μm . A large number of atmospheric absorption peaks are also apparent between 5 and 7 μm , namely from H₂O around 6 μm .

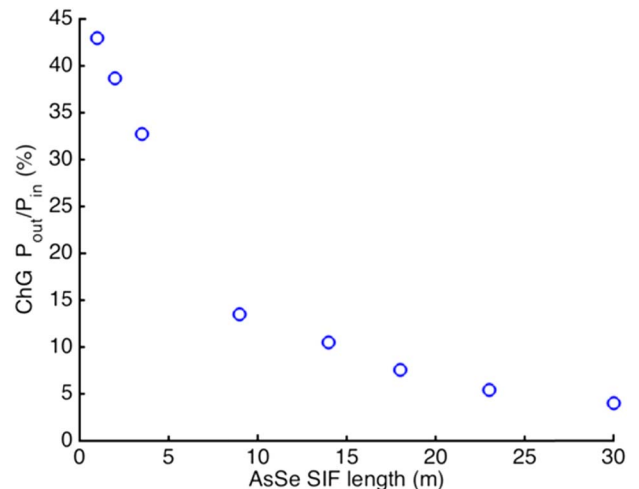


Fig. 5. ChG output/input power ratio as a function of fiber length. The input power is 4.63 mW (0.82 W pump power).

The spectral broadening in the 3.5 m ChG fiber was then investigated as a function of pumping power, as shown in Fig. 6. The IR edge shifts for every pump step, until a pump power of 0.82 W is reached. At this pump level, the average SC power is 1.51 mW, and the spectrum covers the 3–8 μm spectral range. For pump powers up to 0.38 W, the SC average output power displays a steady increase. However, above this pump level, the average output power saturates—a combined effect of the increased losses in the ChG fiber but, more importantly, because the Er:ZFG amplifier's output power saturates as the spectrum is broadened close to the ZFG transparency limit.

Several improvements can be considered for the experimental setup. In a short-term perspective, ChG SIF design optimization to limit confinement losses is of key importance since it is the root cause of the 8 μm loss edge. This could be achieved by increasing the NA and lowering the core diameter to preserve the same cutoff wavelength. A low cutoff wavelength (around 5 μm) is important to ensure high beam quality. The amplifier part of the system could also be optimized to enhance the broadening process in the ChG fiber. In particular, the Er:ZFG fiber length should be optimized to avoid early saturation of the pre-SC, which affects the maximum power that can be extracted from the amplifier. Changing the amplifier glass material, such as by using an erbium-doped IFG, could also be an interesting way to improve the SC performance by extending the pre-SC up to 5.5 μm [12].

For practical applications, it is also critical to increase the average power of the SC. For instance, it is established that a 15–20 mW SC covering the 2–10 μm band would be suitable for optical biopsy [17]. This requirement could be met by scaling the seed's repetition rate from 2 to 20 kHz. For infrared countermeasures, however, the target is a watt-level average power range [18], which is 2 orders of magnitude higher than the current results. The repetition rate of the seed source will have to be increased by the same orders of magnitude, and the losses of the system will have to be lowered significantly. A large portion of the system's losses currently arise from the high Fresnel reflections of our ChG SIF tips.

In the longer-term perspective, an all-fiber scheme (i.e., without free-space components) is the ultimate goal, thereby

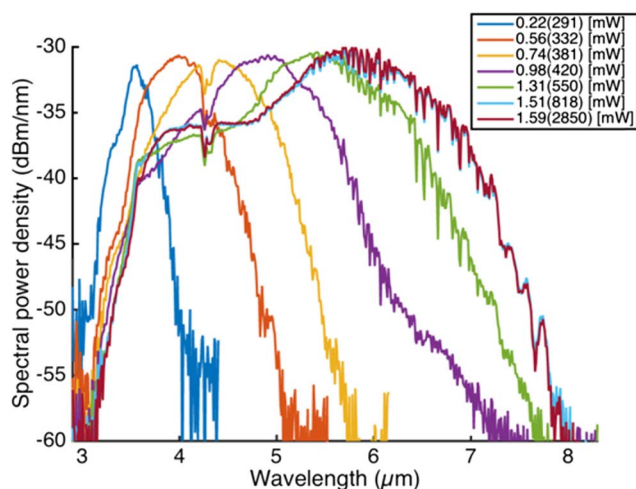


Fig. 6. Evolution of the SC spectrum generated with a ChG fiber length of 3.5 m at different output powers. Corresponding launched pump powers are shown in parentheses.

improving the source's robustness and long-term reliability. In order to achieve this, low-loss fluoride–ChG fusion splices must be developed. Recently, important progress was made by the Naval Research Laboratory (NRL) as they succeeded in making the first repeatable silica–ChG splices [19]. In addition, the development of an all-fiber long-pass filter at the output of the in-amplifier source, for example by using a tilted fiber Bragg grating (FBG) directly written in the ZFG fiber [20], is also an important milestone to reach for enabling the development of such an all-fiber architecture.

In conclusion, an innovative and simple SC source emitting up to 8 μm with 1.5 mW average output power is reported. Such results demonstrate the capabilities of the ZFG in-amplifier pumping source as well as the maturity of AsSe SIF's technology. By performing some improvements to this mid-IR SC setup, a watt-level and all-fiber SC spanning up to 12 μm is within reach.

Funding. Canada Foundation for Innovation (CFI) (5180); Fonds de recherche du Québec—Nature et technologies (FRQNT) (144616); Natural Sciences and Engineering Research Council of Canada (NSERC) (IRCPJ469414-13).

REFERENCES

1. A. B. Seddon, *Phys. Status Solidi B* **250**, 1020 (2013).
2. R. Su, M. Kirillin, E. W. Chang, E. Sergeeva, S. H. Yun, and L. Mattsson, *Opt. Express* **22**, 15804 (2014).
3. G. Tao, H. Ebendorff-Heidepriem, A. M. Stolyarov, S. Danto, J. V. Badding, Y. Fink, J. Ballato, and A. F. Abouraddy, *Adv. Opt. Photon.* **7**, 379 (2015).
4. Y. Tang, F. Li, and J. Xu, *Laser Phys.* **26**, 055402 (2016).
5. T. Cheng, K. Nagasaka, T. H. Tuan, X. Xue, M. Matsumoto, H. Tezuka, T. Suzuki, and Y. Ohishi, *Opt. Lett.* **41**, 2117 (2016).
6. C. R. Petersen, U. Møller, I. Kubat, B. Zhou, S. Dupont, J. Ramsay, T. Benson, S. Sujecki, N. Abdel-Moneim, Z. Tang, D. Furniss, A. Seddon, and O. Bang, *Nat. Photonics* **8**, 830 (2014).
7. H. Ou, S. Dai, P. Zhang, Z. Liu, X. Wang, F. Chen, H. Xu, B. Luo, Y. Huang, and R. Wang, *Opt. Lett.* **41**, 3201 (2016).
8. R. R. Gattass, L. Brandon Shaw, V. Q. Nguyen, P. C. Pureza, I. D. Aggarwal, and J. S. Sanghera, *Opt. Fiber Technol.* **18**, 345 (2012).
9. C. R. Petersen, P. M. Moselund, C. Petersen, U. Møller, and O. Bang, *Opt. Express* **24**, 749 (2016).
10. P. Toupin, L. Brilland, D. Mechin, J. L. Adam, and J. Troles, *J. Lightwave Technol.* **32**, 2428 (2014).
11. J.-C. Gauthier, V. Fortin, S. Duval, R. Vallée, and M. Bernier, *Opt. Lett.* **40**, 5247 (2015).
12. J.-C. Gauthier, V. Fortin, J.-Y. Carrée, S. Poulain, M. Poulain, R. Vallée, and M. Bernier, *Opt. Lett.* **41**, 1756 (2016).
13. C. Agger, C. Petersen, S. Dupont, H. Steffensen, J. K. Lyngsø, C. L. Thomsen, J. Thøgersen, S. R. Keiding, and O. Bang, *J. Opt. Soc. Am. B* **29**, 635 (2012).
14. www.coractive.com.
15. H. G. Dantanarayana, N. Abdel-Moneim, Z. Tang, L. Sojka, S. Sujecki, D. Furniss, A. B. Seddon, I. Kubat, O. Bang, and T. M. Benson, *Opt. Mater. Express* **4**, 1444 (2014).
16. www.lumerical.com.
17. A. B. Seddon, T. M. Benson, S. Sujecki, N. Abdel-Moneim, Z. Tang, D. Furniss, L. Sojka, N. Stone, N. Jayakrupakar, G. R. Lloyd, I. Lindsay, J. Ward, M. Farries, P. M. Moselund, B. Napier, S. Lamrini, U. Møller, I. Kubat, C. R. Petersen, and O. Bang, *Proc. SPIE* **9703**, 970302 (2016).
18. H. H. P. T. Bekman, J. C. van den Heuvel, F. J. M. van Putten, and R. Schleijsen, *Proc. SPIE* **5615**, 27 (2004).
19. R. Thapa, R. R. Gattass, V. Nguyen, G. Chin, D. Gibson, W. Kim, L. B. Shaw, and J. S. Sanghera, *Opt. Lett.* **40**, 5074 (2015).
20. M. Bernier, D. Faucher, R. Vallée, A. Salimonia, G. Androz, Y. Sheng, and S. L. Chin, *Opt. Lett.* **32**, 454 (2007).